Empirical constraints on the $^{16}O + {}^{40}Ca$ optical potential

S. Krewald, A. Djaloeis, and S. Gopal
Institut für Kernphysik, Kernforschungsanlage Jülich, D-5170 Jülich, West Germany
(Received 6 April 1981)

The angular distribution between $20° \lesssim \theta_{c.m.} \lesssim 180°$ of $^{16}O + {}^{40}Ca$ elastic scattering at $E_{c.m.} = 35.7$ MeV has been analyzed in terms of the optical model. For both the real and imaginary parts, the standard Woods-Saxon and spline-function parametrizations of the optical potential have been investigated. In the angular region $\theta_{c.m.} \lesssim 112°$, Woods-Saxon – Woods-Saxon potential combinations suffice to describe the data; however, no fit could be obtained either by Woods-Saxon – Woods-Saxon or by Woods-Saxon – Spline-function potentials for the complete angular distribution ($\theta_{c.m.} \lesssim 180°$). In contrast, the Spline-function – Woods-Saxon combination reproduces the experimental data well. No further improvement of fit quality is obtained by parametrizing both the real and imaginary parts in terms of spline functions. The best-fit Spline-function – Woods-Saxon potential is found to consist of a real part, having significant wiggles in the interior, coupled to a shallow imaginary part with a depth $W \sim 2$ MeV and a large radius $R_i = 1.60(A_P^{1/3} + A_T^{1/3})$ fm.

[NUCLEAR REACTIONS $^{16}O + {}^{40}Ca$ elastic scattering, $E_{c.m.} = 35.7$ MeV; optical model analysis including a "model-independent" potential parametrization by spline functions.]

I. INTRODUCTION

In analogy to the light ion ($A_P \lesssim 3$) case, the description of the elastic scattering of a heavy ion has been generally attempted in terms of the optical model. Analyses performed so far have given inconsistent pictures regarding how far the elastic scattering data could give information on the potential shape, particularly, in the interior region. For example, using the notch perturbation method, Cramer and DeVries[1] have found that neither light- nor heavy-ion scattering at any energy probes the interior of the nucleus. On the other hand, using a similar method, Delbar *et al.*[2] have shown that angular distributions for the α -particle elastic scattering on $^{40,44}Ca$ nuclei at $E_\alpha = 36.2$ MeV are influenced not only by the tail region of the potential, but also by the very inner part around $R = 2$ fm. In fact, the details of the potential shape in the interior region were found to be responsible for the so-called "anomalous large angle scattering" (ALAS) observed in $^{40}Ca(\alpha,\alpha)$ elastic scattering.[3–5] It is worth mentioning that deep penetration ("transparency") of α particles into the ^{40}Ca nucleus was also suggested by Friedman and Batty[6] from their model-independent analysis of $\alpha + {}^{40}Ca$ elastic scattering at $E_\alpha = 140$ MeV. Taking advantage of this transparency of ^{40}Ca to α particles, Michel and Vanderpoorten[5] succeeded at obtaining a consistent description of α-^{40}Ca elastic scattering over a wide range of incident energies using a "spline-parametrization" technique.

It is well known that a phenomenon similar to the ALAS has also been observed[7–9] in some heavy-ion elastic scatterings. Attempts to explain this phenomenon in terms of, e.g., quasimolecular resonance, the cluster exchange mechanism, or simple potential scattering have been summarized in Ref. 10. While enhancement of the large-angle cross section can be obtained easily with a conventional optical model potential having Woods-Saxon shape in both real and imaginary parts by simply reducing the strength of the imaginary potential,[11] the details of the angular distribution cannot be reproduced correctly.

In this report, we present results of an optical model analysis of $^{16}O + {}^{40}Ca$ elastic scattering at $E_{c.m.} = 35.7$ MeV, measured up to $\theta_{c.m.} = 180°$.[9] The objectives are (1) to check whether a better description of the experimental angular distribution can be obtained by giving more degrees of freedom to the real and/or imaginary part of the optical potential, and (2) to see to what extent the ^{40}Ca nucleus can be transparent to an ^{16}O projectile which is considered to consist of α clusters; in particular, to establish whether the elastic scattering cross sec-

tion is also sensitive to the details of the optical potential in the interior region.

II. METHOD OF ANALYSIS

The optical model analysis was performed using the computer code "OPTY,"[12] which automatically searches for the optimum values of the potential parameters by minimizing the χ^2 value defined as

$$\chi^2(a_1,\ldots,a_M) = \frac{1}{F}\sum_i \left[\frac{\sigma_{\exp}(\theta_i) - \sigma_{\text{th}}(\theta_i,a_1,\ldots,a_M)}{\Delta\sigma_{\exp}(\theta_i)}\right]^2 .$$

At each angle θ_i, the quantities $\sigma_{\exp}(\theta_i)$, $\Delta\sigma_{\exp}(\theta_i)$, and $\sigma_{\text{th}}(\theta_i)$ represent the experimental value, its estimated error, and the theoretical value of the elastic scattering differential cross sections, respectively. The potential parameters searched upon are denoted by $a_1,\ldots,a_M$; the quantity F represents the number of degrees of freedom.

For the spline parametrization, the starting spline parameters S_i ($i = 1,\ldots,M$; $M = 12$) at the corresponding radii r_i were computed from the potential sets SA, ST1, and ST2 (strong absorption, and surface transparent 1 and 2, respectively) of Ref. 9 (see Table I). Several sets of r_i values, among which a set with $r_i = (i - 1)$ fm, $i = 1, \cdots, 12$, were used to study the dependence of the resulting best-fit potential (see Sec. III) on the starting conditions of the search procedure.

The error band associated with the extracted best-fit spline real potential was calculated using the covariant matrix method as described in Ref. 6. It should be emphasized that this error band reflects only the statistical uncertainties of the extracted potential shape around the χ^2 -miminum value.

III. RESULTS

Figure 1 shows the experimental angular distribution relative to the Rutherford cross section. The dashed curve denotes the optical model prediction using the Woods-Saxon–Woods-Saxon (WS-WS) potential set ST1 of Ref. 9. The best-fit curve obtained in this work using a spline-function–Woods-Saxon (SPL-WS) potential is given by the solid line (see Table I).

It can be seen from Fig. 1 that the SPL-WS potential gives far better fit quality compared to that obtained using ST1, in particular at angles $\theta_{\text{c.m.}} \gtrsim 112°$, where the ST1 curve drastically disagrees with experiment. It should be recalled that the sets ST1 and ST2 of Ref. 9 are characterized by a weak imaginary potential which was required to produce an oscillatory pattern at angles $\theta_{\text{c.m.}} \gtrsim 112°$ (see Fig. 2). This feature was also found by Satchler[11] in the analysis of the $^{16}O + ^{28}Si$ elastic scattering data at $E_{\text{c.m.}} \sim 33$ MeV. We have also performed further searches using WS-WS potentials. We confirmed that the use of a strong imaginary part does not produce an oscillatory pattern in the angular distribution at large angles for both WS and SPL parametrizations of the real part of the potential. For a WS real part, no further improvement was obtained even after giving more degrees of freedom to the imaginary potential by using a spline function. Similarly, the use of a spline parametrization of both the real and imaginary parts did not bring any significantly better fit quality than that represented by the solid line in Fig. 1.

Figure 2 shows the radial dependence of the real and imaginary potentials used in the present work and those of Ref. 9. The parameters are listed in Table I. The following features are worth noting:

TABLE I. The $^{16}O + ^{40}Ca$ optical potential parameters for $E_{\text{c.m.}} = 35.7$ MeV. Radii are defined as $R = r(A_P^{1/3} + A_T^{1/3})$ and $r_c = 1.0$.

Set	V (MeV)	r_r (fm)	a_r (fm)	W (MeV)	r_i (fm)	a_i (fm)	Ref.
SA	10.01	1.364	0.616	23.38	1.289	0.535	9
ST1	24.76	1.403	0.399	3.80	1.281	0.221	9
ST2	50.00	1.329	0.420	7.60	1.000	0.300	9
SPL-WS	spline[a]	spline[a]	spline[a]	2.16	1.601	0.155	present
SPLA	spline[a]	spline[a]	spline[a]	2.16	1.601	0.155	present

[a]See Fig. 2.

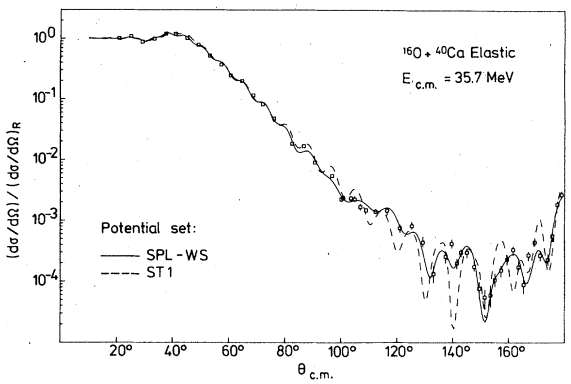

FIG. 1. The experimental angular distribution of the $^{16}O + ^{40}Ca$ elastic scattering at $E_{c.m.} = 35.7$ MeV relative to the Rutherford cross section. The solid line represents the best-fit obtained in the present work using a SPL-WS potential (see text); the dashed curve was calculated using the potential set ST1 of Kubono *et al.*[9] (Ref. 9).

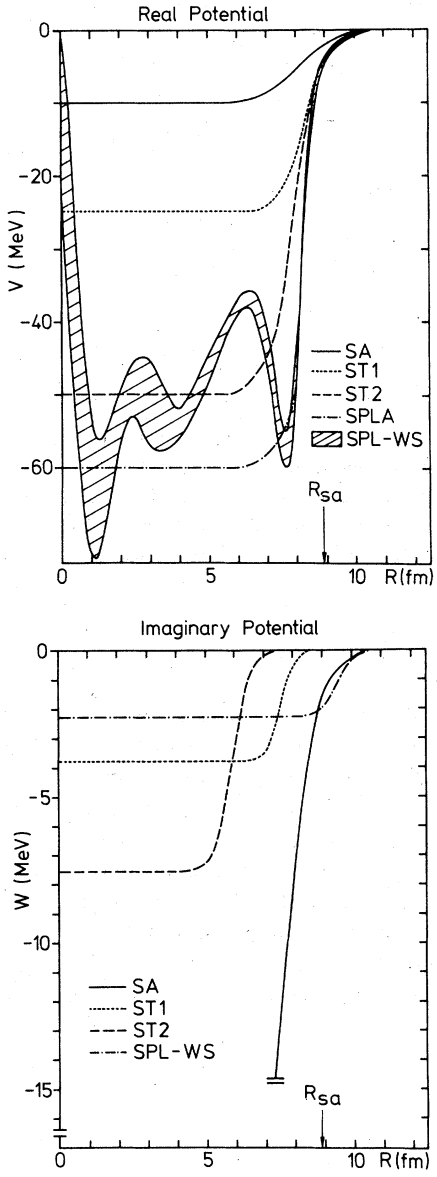

FIG. 2. The radial dependence of both the real and imaginary parts of the best-fit SPL-WS potential compared to those obtained in Ref. 9.

(i) The real part of the best-fit SPL-WS potential exhibits significant wiggles in the interior region, similar to those observed by Barrette and Kahana[10] in the analysis of $^{16}O + ^{28}Si$ elastic scattering angular distribution at $E_{c.m.} = 21.2$ MeV. The effects of using different sets of radii r_i were investigated and not found to change the conclusion.

(ii) The best-fit imaginary potential is found to have a depth of only about 2 MeV but having a large range with a radius $R_i = 1.6(A_P^{1/3} + A_T^{1/3})$ fm. This result corroborates those found by Satchler[11] and Mackintosh *et al.*[13] In the interior region, this depth is much smaller than that of the sets ST1 and ST2 of Kubono *et al.*[9] However, in the surface region near the strong absorption radius $R_{SA} = 1.5(A_P^{1/3} + A_T^{1/3})$ fm (see Fig. 2), ST1 and ST2 give practically no absorption, whereas in the SPL-WS potential the absorption strength resembles that of the strong absorption potential set SA. It is worthwhile to point out (see Figs. 1 and 2) that the experimental data in the angular range $\theta_{c.m.} \lesssim 112°$ do not put strong constraints on the geometry of the imaginary potential. Good fits of comparable quality are obtained either with the set SA (strong absorption potential) or with the extremely surface transparent potential ST1 which reaches its full absorption strength only in the region far inside of the strong absorption radius.

The influence of the absorption strength on the theoretical angular distribution in the present best-fit potential is illustrated in Fig. 3. It can be seen that a strong oscillatory structure is observed in the absence of absorption. Furthermore, the absorptive potential clearly plays an essential role for the overall reduction of the cross sections at large angles, as well as for modifying the oscillatory pattern. The fact that an imaginary depth of only about 2 MeV is necessary to describe the experimental angular distribution satisfactorily suggests, as in the $\alpha + ^{40}$ Ca system,[2] a high degree of transparency of the ^{40}Ca nucleus to the incoming ^{16}O projectile. This finding contradicts the claim put by the authors of Ref. 1 that neither light- nor heavy-ion

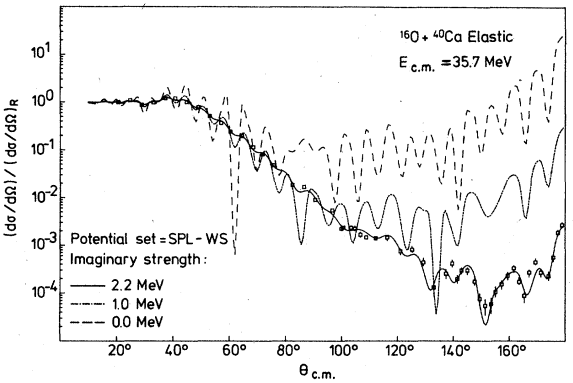

FIG. 3. Illustration of the sensitivity of the optical model cross section with respect to the variation of the depth in the imaginary part of the best-fit SPL-WS potential ($W = 0$ MeV, dashed line; $W = 1$ MeV, dotted-dashed line; best-fit SPL-WS, solid line).

scattering at any energy probes the interior of the nucleus.

Figure 4 shows the effects of modifying only the interior shape of the real potential on the angular distribution. The dashed curve is obtained using the real potential SPLA (see Fig. 2) obtained from the SPL set by modifying it to have a smooth shape in the region $R \leq 8$ fm. The angular distribution is strongly affected in the large angle region ($\theta_{c.m.} \gtrsim 112°$), the resulting curve being in gross disagreement with the data. In this analysis the wiggle structure in the interior region of the real potential

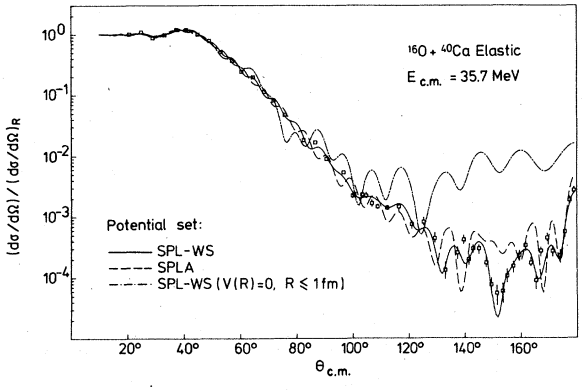

FIG. 4. Illustration of the sensitivity of the optical model cross section with respect to changes in the radial dependence of the real part of the $^{16}O + {}^{40}Ca$ optical potential (see text). Dashed line: potential set SPLA of Fig. 2; dotted-dashed line: best-fit SPL-WS potential cutoff at $R = 1$ fm; solid line: best-fit SPL-WS potential.

does indeed appear to be necessary to describe the back-angle data correctly. In order to assess the possible physical significance of the wiggles, one should note that the optical potential for the scattering of two composite particles is a highly nonlocal quantity.[14] The conventional analysis is heavy ion scatterings in terms of the optical model has, to date, relied only on local potentials. One should, therefore, ask what the shape of an equivalent local potential should take. This question has been studied recently by Bauhoff *et al.*[15] for the case of proton scattering from ^{12}C and ^{40}Ca. They have constructed an equivalent local potential containing no singularities from the regular and the irregular solutions of the nonlocal scattering problem. In the case of 30 MeV protons, the equivalent local potential resembles a WS shape only in the surface region; the interior part, however, exhibits rapid oscillations. In view of this, we suggest that the wiggles in the real part of the present best-fit potential may be due to the nonlocality of the heavy-ion potential. Indeed, nonlocality effects for the $^{16}O + {}^{40}Ca$ system due to the Pauli principle have been taken into account by Friedrich *et al.*[16] using a one-channel approximation to the resonating group method. A strong backward rise in the angular distribution was predicted for $E_{c.m.} = 30$ MeV, which qualitatively agrees with the currently analyzed data at $E_{c.m.} = 35.7$ MeV.

Finally, to test the sensitivity of the predicted cross section to the deep interior region of the real potential, we modified the SPL potential by setting the potential value for zero for $R \leq 1$ fm. The resulting angular distribution is shown in Fig. 4 (dotted-dashed curve). The large angle cross sections are strongly affected, a feature similar to that found by Delbar *et al.*[2]

IV. CONCLUSIONS

From the present model-independent analysis of the $^{16}O + {}^{40}Ca$ elastic scattering angular distribution at $E_{c.m.} = 35.7$ MeV the following conclusions can be drawn:

(i) Fixing the analytic form of the real potential to a WS shape cannot lead to a good description of the experimental data.

(ii) On the other hand, the data are successfully described by a spline real potential in combination with either a WS or a spline imaginary part. However, no significant improvement is obtained by giving more freedom (through a spline parametrization)

to the imaginary part.

(iii) The best-fit SPL-WS potential is characterized by a real part having an oscillatory pattern in the interior region and by a shallow ($W \sim 2$ MeV) imaginary potential with a large radius $R_i = 1.6$ $(A_P{}^{1/3} + A_T{}^{1/3})$ fm. The theoretical cross sections are found to be sensitive to the depth of the imaginary potential as well as to the shape of the interior part of the real potential.

In order to assess the significance of the present results, the following steps are necessary:

(i) Consistency checks should be performed by analyzing experimental data which cover a large angular range at other incident energies. However, no such data $^{16}O + {}^{40}Ca$ are available at present.

(ii) It is extremely important to check theoretically whether the oscillatory structure in the interior region of the real potential is indeed due to the nonlocality of the $^{16}O + {}^{40}Ca$ optical potential.

One of the authors (S.G.) would like to sincerely thank Professor C. Mayer-Böricke for providing an opportunity to stay in Jülich.

[1]J. G. Cramer and R. M. DeVries, Phys. Rev. C 22, 91 (1980).
[2]T. Delbar *et al.*, Phys. Rev. C 18, 1237 (1987).
[3]D. M. Brink and N. Takigawa, Nucl. Phys. A279, 159 (1977).
[4]H. P. Gubler *et al.*, Phys. Lett. 74B, 202 (1978).
[5]F. Michel and R. Vanderpoorten, Phys. Lett. 82B, 183 (1979).
[6]E. Friedman and C. J. Batty, Phys. Rev. C 17, 34 (1978).
[7]C. K. Gelbke *et al.*, Phys. Rev. Lett. 41, 1778 (1978).
[8]P. B. Munzinger *et al.*, Phys. Rev. Lett. 38, 944 (1977).
[9]S. Kubono, P. D. Bond, and C. E. Thorn, Phys. Lett. 81B, 140 (1979).
[10]J. Barrette and S. Kahana, Comments Nucl. Part. Phys. 9, 67 (1980).
[11]G. R. Satchler, Nucl. Phys. A329, 233 (1979).
[12]H. Dabrowski, R. Planeta, and A. Djaloeis, IKP-KFA Jülich, Report 1637, 1980.
[13]R. S. Mackintosh and A. M. Kobos, Phys. Lett. 92B, 59 (1980).
[14]H. Feshbach, Ann. Phys. (N.Y.) 5, 287 (1962).
[15]W. Bauhoff, H. V. v. Geramb, and G. Pálla (unpublished).
[16]H. Friedrich, K. Langanke, and A. Weiguny, Phys. Lett. 63B, 125 (1976).